Earth and Planetary Science Letters 394 (2014) 159–167

Contents lists available at ScienceDirect

Earth and Planetary Science Letters

www.elsevier.com/locate/epsl

A role for scavenging in the marine biogeochemical cycling of zinc and zinc isotopes

Seth G. John *, Tim M. Conway

Department of Earth and Ocean Sciences, University of South Carolina, Columbia, SC 29208, USA

ARTICLE INFO

Article history:
Received 23 August 2013
Received in revised form 21 February 2014
Accepted 28 February 2014
Available online 2 April 2014
Editor: G.M. Henderson

Keywords:
GEOTRACES
zinc
cadmium
isotopes
North Atlantic
NAZT

ABSTRACT

Zinc (Zn) and cadmium (Cd) are important biologically active trace-metals in the ocean. To date, the marine distributions of these elements have been understood primarily in terms of biological assimilation by growing phytoplankton and regeneration of sinking biological material. Initial studies of Zn and Cd concentrations and stable isotope ratios (δ^{66}Zn and δ^{114}Cd) have therefore focused on their use as simple tracers of assimilation and regeneration in the oceans. However, these two processes are insufficient to explain new data on the marine distribution of Zn and δ^{66}Zn. Here, using the first high-resolution paired marine depth profiles of Zn, Cd, δ^{66}Zn and δ^{114}Cd, we suggest that scavenging of Zn onto organic matter plays a major, yet largely unconsidered, role in the marine cycling of Zn. This hypothesis is supported by culture experiments, which show that Zn released from degrading phytoplankton is rapidly scavenged back onto organic matter, and that adsorbed Zn is isotopically heavier than the dissolved phase by 0.58‰. In contrast, very little Cd or phosphate was scavenged and Cd isotopes were not significantly fractionated during degradation. Our hypothesis is further supported by one-dimensional modeling, which reproduces observed marine δ^{66}Zn profiles with <1% of Zn adsorbed to particles. Understanding how Zn cycling in the oceans is a balance between assimilation, scavenging, and regeneration is necessary in order to investigate δ^{66}Zn as a tracer of marine productivity. We anticipate that paired analyses of δ^{66}Zn and δ^{114}Cd will prove to be valuable new tools in constraining patterns of global primary productivity, providing key information for the marine carbon cycle during periods of past and present global climate change.

1. Introduction

Zn and Cd show nutrient-like distributions in the oceans, with surface depletion attributed to phytoplankton growth and gradual enrichment in deeper waters from dissolving organic material. Proxies for Zn and Cd and their stable isotope ratios have therefore been used to infer changes in biological productivity and circulation in the past ocean. For example, seawater Zn and Cd concentrations, as recorded in carbonate Zn/Ca or Cd/Ca, have been used to reconstruct paleonutrient distributions (Boyle, 1992; Marchitto et al., 2005, 2002). δ^{66}Zn variations of 1‰ in a sedimentary carbonate record from the Equatorial Pacific were attributed to productivity changes over the past 175 kyr (Pichat et al., 2003). Similarly, δ^{66}Zn variations in Ediacaran carbonates were attributed to changes in biological productivity following the Marinoan 'Snowball Earth' glaciation (Kunzmann et al., 2013). As new analytical techniques for δ^{66}Zn and δ^{114}Cd are developed, we anticipate greater use of isotopes as tracers for past global change.

Although Zn and Cd are chemically similar elements, they have different marine distributions. Globally, the marine distribution of Zn is similar to the major nutrient silicate (Si), while the distribution of Cd is similar to the major nutrients nitrate (N) and phosphate (P). Zn and Si have deeper 'regeneration maxima' than N, P and Cd, and both Si and Zn are enriched 5- to 8-fold in the deep North Pacific compared to the deep North Atlantic, while N, P and Cd are enriched only about 3-fold at similar locations (Sunda, 2012). As with the marine distribution of Zn and Cd, the distribution of δ^{66}Zn, and δ^{114}Cd in the ocean have been attributed to active biological uptake (assimilation) of these metals by phytoplankton at the surface, and release (regeneration) of these metals from sinking biological particles. In culture, phytoplankton have been shown to fractionate Zn and Cd isotopes during assimilation due to the preferential uptake of lighter isotopes (John et al., 2007; Lacan et al., 2006). A biological preference for lighter Cd and Zn isotopes has similarly been invoked to explain increasing δ^{66}Zn and δ^{114}Cd towards the surface of the ocean (Bermin et al., 2006;

* Corresponding author. Tel.: +1 803 777 7052.
E-mail address: sjohn@geol.sc.edu (S.G. John).

http://dx.doi.org/10.1016/j.epsl.2014.02.053
0012-821X/

Lacan et al., 2006; Ripperger et al., 2007). A correlation between surface productivity and manganese nodule δ^{66}Zn has also been attributed to biological Zn fractionation (Maréchal et al., 2000), though the precise mechanism of this correlation is unclear. Finally, variations in diatom frustule δ^{66}Zn in Southern Ocean core-top sediments are consistent with biological preferential assimilation of light Zn isotopes in surface waters (Andersen et al., 2011), though more recent measurements of seawater dissolved δ^{66}Zn do not show a strong correlation between Zn uptake and increasing δ^{66}Zn (Zhao et al., 2014).

Despite the use of δ^{66}Zn as a tracer for biological productivity, the biological cycling of Zn is not fully understood. It has been hypothesized that the similarity between Zn and Si distributions is caused by the presence of Zn in a refractory phase that is similarly resistant to dissolution as diatom opal (e.g. Lohan et al., 2002). However, most Zn in diatoms, from both open-ocean and culture studies, is present in the soft tissue of phytoplankton, as determined by the spatial co-location of Zn with P, rather than Si (Twining et al., 2004, 2003). Only ~1–3% of diatomaceous Zn was found to be present in diatom opal (Ellwood and Hunter, 2000), though additional Zn is present associated with organic material in the frustules (e.g. Pokrovsky et al., 2005). The majority of intracellular Zn in carbon-limited diatom cells is thought to be present in carbonic anhydrase and alkaline phosphatase enzymes under conditions of carbon or phosphate limitation, respectively (Morel et al., 1994; Shaked et al., 2006). If Zn is largely located in the active site of enzymes, then Zn should remineralize at the same rate as N, P and Cd. An alternative explanation for the global similarity between Zn and Si concentrations is that both may be controlled by similar rates of biological assimilation in the surface of the Southern Ocean. Rapid uptake of Si by diatoms in the Southern Ocean has been invoked to explain the deficit of Si compared to N (negative Si*) in the thermocline throughout the oceans (Sarmiento et al., 2004). By analogy, a relatively rapid uptake of Zn in the surface of the Southern Ocean may contribute to the Zn deficit, compared to N, P, and Cd, in the thermocline at lower latitudes; despite this, even models which stress the importance of assimilation in the surface Southern Ocean do not discount the potential importance of slow silicate redissolution on the global distribution of Si (Sarmiento et al., 2007). We are therefore motivated to seek possible reasons why Zn might dissolve more deeply in the water column than other nutrient elements such as N, P, and Cd.

Most prior studies have not considered scavenging, or have not found a significant role for scavenging influencing the distribution of Zn in the oceans. Experiments on degrading marine biogenic material confirm that Zn is released from particles more slowly than N, P or Cd (Collier and Edmond, 1984; Lee and Fisher, 1992). However, these experiments only measured the net rate at which elements were released into the dissolved phase, and did not attempt to quantify the importance of readsorption or scavenging. Scavenging of Zn is thought to explain the high Zn:P ratios observed in South China Sea sediment traps (Ho et al., 2010, 2007), though most Zn in this region is delivered from anthropogenic aerosols, limiting applicability of this study to the open ocean. A 1-dimensional model with Zn input at the surface ocean and reversible-scavenging, similar to models originally developed for short residence elements such as Th and Pa (Bacon and Anderson, 1982), did not reproduce the global distribution of Zn (Little et al., 2013). However, given that this model did not include circulation, and the residence time of Zn in the ocean is much greater than the overturning of the ocean (~50,000 years compared to ~2000 years; Shiller and Boyle, 1985), the misfit between the model and data does not preclude a role for scavenging. Zn scavenging may play a role in Zn biogeochemical cycling in conjunction with other processes, such as biological uptake and remineralization, and ocean mixing and circulation.

Here, we explore the degree to which readsorption onto sinking particles (scavenging) could influence the marine biogeochemical cycling of Zn, using Zn and Cd distribution and isotopic data from the North Atlantic, data from degrading phytoplankton cultures, and a simple 1-D model.

2. Methods

2.1. Sample collection and analysis

Seawater samples were collected on the US GEOTRACES A03 North Atlantic Zonal transect cruises in 2010 and 2011 at stations USGT10-9 (17.3° N, 18.3° W, Oct. 27th 2010), USGT10-10 (17.3° N, 20.8° W, Oct. 30th 2010), USGT11-10 (31.8° N, 64.2° W, Nov. 20, 2011), USGT11-12 (29.7° N, 56.8° W, Nov. 23th 2011) and USGT11-18 (24.1° N, 40.2° W Dec. 2nd 2011). Samples were collected using the US GEOTRACES trace-element clean carousel and filtered (0.4 µm) in a purpose-built clean van (Cutter and Bruland, 2012). Seawater dissolved Zn and Cd concentration, δ^{66}Zn and δ^{114}Cd were measured on a Thermo Neptune MC-ICPMS at the Centre for Elemental Mass Spectrometry at the University of South Carolina, with a double spike technique, after extraction onto Nobias PA-1 resin and purification by anion exchange chromatography following previously published methods (Conway et al., 2013).

Stable isotope ratios are presented as δ^{66}Zn or δ^{114}Cd where:

$$\delta^{66}\mathrm{Zn} = \left(\frac{(\frac{^{66}\mathrm{Zn}}{^{64}\mathrm{Zn}})_{sample}}{(\frac{^{66}\mathrm{Zn}}{^{64}\mathrm{Zn}})_{JMC}} - 1 \right) \times 1000 \quad (1)$$

and

$$\delta^{114}\mathrm{Cd} = \left(\frac{(\frac{^{114}\mathrm{Cd}}{^{110}\mathrm{Cd}})_{sample}}{(\frac{^{114}\mathrm{Cd}}{^{110}\mathrm{Cd}})_{NIST\text{-}3108}} - 1 \right) \times 1000. \quad (2)$$

For culturing experiments, the difference between two phases is given by:

$$\Delta\delta Y_{A-B} = \delta Y_A - \delta Y_B$$

for the two phases A and B (e.g. phytoplankton cells and the media in which they were grown).

2.2. Culture experiments

Cultures were grown and processed for isotope analysis in the MTEL laboratories at the University of South Carolina under ULPA-filtered air flow using acid-cleaned labware, ultrapure water (>18.2 MΩ) and distilled high purity acids. The marine flagellate chlorophyte *Dunaliella tertiolecta* was grown for several months under non-axenic conditions, in $f/2$ medium prepared with 0.2 µm filtered seawater from the Baruch Marine Field Laboratory in Georgetown, SC. For our experiments, cells were transferred into a modified AQUIL media (Morel et al., 1979) containing 10^{-4} M EDTA (Sunda et al., 2005) with a ~100-fold increase in Zn concentrations (10^{-5} M) compared to AQUIL and with the addition of Cd (10^{-6} M), in order to increase the quantity of these metals within the cells. Additionally, Fe concentrations were reduced 10-fold (10^{-7} M) compared to AQUIL in order to minimize cell-surface precipitation of metals, as Zn has been observed to co-precipitate with Fe oxyhydroxides on cell surfaces in media with high Fe concentrations (10^{-5} M) (John et al., 2007) but does not precipitate in similar media with lower Fe concentrations (10^{-6} M) (Sunda and Huntsman, 1992). The media free-inorganic ion concentrations of Zn and Cd (Zn' and Cd') were $1.5 \cdot 10^{-9}$ M and $5.9 \cdot 10^{-9}$ M, respectively, and the divalent ion concentrations (Zn^{2+} and Cd^{2+}) were $1.0 \cdot 10^{-9}$ M and $1.7 \cdot 10^{-10}$ M, respectively, as calculated using the equations of Sunda et al. (2005).

D. tertiolecta was cultured for >10 generations in the modified-AQUIL media before 0.1% inoculation into a 4 L bottle for experiments. The 4 L culture was grown to the end of log-phase growth, at which point 1% of the media Zn and 2.5% of the Cd had been taken up into the cells (Table S1). Cells were concentrated from 1 L of media by centrifugation, rinsed twice by resuspending in metal-free chelexed artificial seawater (no added nutrients, trace-metals, or EDTA) then centrifugation, then resuspended in 20 mL metal-free artificial seawater, and finally stored in the dark at 23 °C. At each time point (4 h, 1, 2, 4, 7, 9, and 12 days), 2 mL of the cell suspension was centrifuged and the supernatant was decanted (dissolved fraction). The remaining cells from the 2 mL subsample were resuspended in 1 mL of a pH 8 oxalate-EDTA solution for 20 min to remove any adsorbed trace metals, centrifuged, and the supernatant was decanted (adsorbed fraction). Samples were dried in Savillex PFA vials, heated overnight with 2 mL aqua regia to destroy residual organic material, dried, and redissolved in 1 mL 1 M HCl. A 50 µL subsample was taken for P, Zn, and Cd concentration analysis by Thermo Element II sector field ICPMS, in medium resolution with standard Ni sampler and skimmer cones, by reference to the intensity of these elements in solutions of known concentration. Zn and Cd double-spikes were added to samples in a 1 : 4 ratio (natural : spike) prior to purification by anion exchange chromatography on 135 µL AG-MP1 resin following a procedure modified from Conway et al. (2013) using 800 µL 1 M HCl to elute salts, 1200 µL 2 M HNO_3 + 0.1 M HBr to elute Zn, and 1000 µL 2 M HNO_3 to elute Cd. Samples were analyzed for δ^{66}Zn and δ^{114}Cd as previously described for seawater (Conway et al., 2013). External error for the cell suspension analyses was determined by purifying and analyzing two separate aliquots of the total culture for δ^{66}Zn and δ^{114}Cd, which were equal within analytical error (Table S1).

2.3. Model description

Cd and Zn concentration and isotopic profiles were modeled according to a steady-state 1-dimensional advection–diffusion equation where the concentration of Zn or Cd (C) at any depth in the ocean is given by:

$$\frac{\partial C}{\partial t} = 0 = \kappa \frac{\partial^2 C}{\partial z^2} + JC \tag{3}$$

where κ is the vertical diffusivity and J represents all of the inputs and losses to the dissolved phase from particles. J is therefore the net effect of biological uptake into particles, release from particles due to remineralization, scavenging onto particles, and release of scavenged from particles. Vertical diffusivity was prescribed as 10^{-4} m^2 s^{-1} in a 30 m mixed layer and 10^{-5} m^2 s^{-1} in the thermocline, and did not fractionate isotopes. Biological assimilation was held constant throughout the mixed layer, and decreased in the thermocline from the assumption of exponential decay of photosynthetically active radiation (PAR) with a 1% light level at 30 m so that the rate of assimilation is described as:

$$J_{assimilation} = k_{assimilation} \cdot PAR \cdot C \tag{4}$$

where $k_{assimilation}$ is the rate constant for biological uptake and C is the amount of an isotope of Cd or Zn. Biological assimilation of Zn was parameterized with an isotope effect of $\Delta\delta^{66}Zn_{plankton\text{-}seawater} = -0.2‰$, as was determined for Zn uptake by the high-affinity pathway expected to dominate at seawater [Zn] (John et al., 2007) such that:

$${}^{66}k_{assimilation} = 0.9998 \cdot k_{assimilation} \tag{5}$$

where ${}^{66}k_{assimilation}$ and $k_{assimilation}$ are the rate constants for uptake of ^{66}Zn and ^{64}Zn, respectively. Similarly, Cd assimilation was parameterized with an isotope effect of −0.4‰ based on the biological fractionation of Cd isotopes observed in the Antarctic Circumpolar Current (Abouchami et al., 2011) such that:

$${}^{114}k_{assimilation} = 0.9996 \cdot k_{assimilation}. \tag{6}$$

For Zn only, the rate of scavenging onto organic particles was defined as:

$$J_{scavenging} = k_{scavenging} \cdot [\text{POCd}] \cdot [\text{Zn}] \tag{7}$$

where [POCd] is the concentration of organic Cd at each depth (which is assumed to be proportional to the total concentration of organic particles), and scavenging occurred with the experimentally-determined isotope effect of 0.58‰ so that:

$${}^{66}k_{scavenging} = 1.00058 \cdot k_{scavenging}. \tag{8}$$

Biological remineralization is parameterized according to the logarithmic dissolution of organic material with depth according to the equation:

$$F_z = F_{100} \cdot \left(\frac{z}{100}\right)^b \tag{9}$$

where F_z is the flux at depth z, F_{100} is the flux at 100 m, z is depth, and b is a variable describing the rate at which organic matter remineralizes (Martin et al., 1987). Boundary conditions at 1000 m were held constant at [Cd] = 0.55 nmol kg^{-1}, [Zn] = 2 nmol kg^{-1}, δ^{114}Cd = +0.5‰, and δ^{66}Zn = +0.5‰ based on data from station USGT10-10. The layer model was constructed with 100 layers, each 10 m thick, where for each depth the full version of Eq. (4) includes mixing, loss to biological uptake and scavenging, and inputs from biological remineralization and desorption. Because the rates of remineralization and desorption depend on processes which occur higher in the water column, this yields a set of 100 equations, one for every depth, each of which contains up to 100 unknowns, the Zn concentrations at every depth, solved by matrix inversion in Matlab.

The model was constrained to fit data from station USGT10-10 by minimizing the sum of squared errors between model output and a linear interpolation between data points at depths each 10 m. First, $k_{assimilation}$ was adjusted to fit the observed seawater dissolved δ^{114}Cd profile. Then, b was adjusted to match the observed [Cd] profile. Because these two parameters interact, they were determined iteratively. However, because $k_{assimilation}$ mostly affects δ^{114}Cd in the upper portion of the profile while b mostly affects [Cd] in the lower part of the profile, minimized error in both δ^{114}Cd and [Cd] was achieved after a few iterations. The error between modeled and observed [Zn] was minimized by varying $k_{scavenging}$. Finally, the δ^{66}Zn profile was predicted from the model, without adjusting any further parameters to match observations. Model sensitivity to the choice of isotopic fractionations was tested by varying the biological isotope effects for Cd and Zn assimilation from 0 to −1‰, and varying the isotope effect for scavenging from 0 to +1‰, covering more than the observed range for biological fractionation (Abouchami et al., 2011; John et al., 2007; Lacan et al., 2006) and Zn adsorption to biological material (this study; Gélabert et al., 2006).

3. Results and discussion

3.1. North Atlantic data

Five high-resolution paired profiles of Zn, δ^{66}Zn, Cd and δ^{114}Cd are presented from the US GEOTRACES North Atlantic Zonal A03 Transect (USGT10 and 11; Fig. 1). In all profiles, Cd concentrations

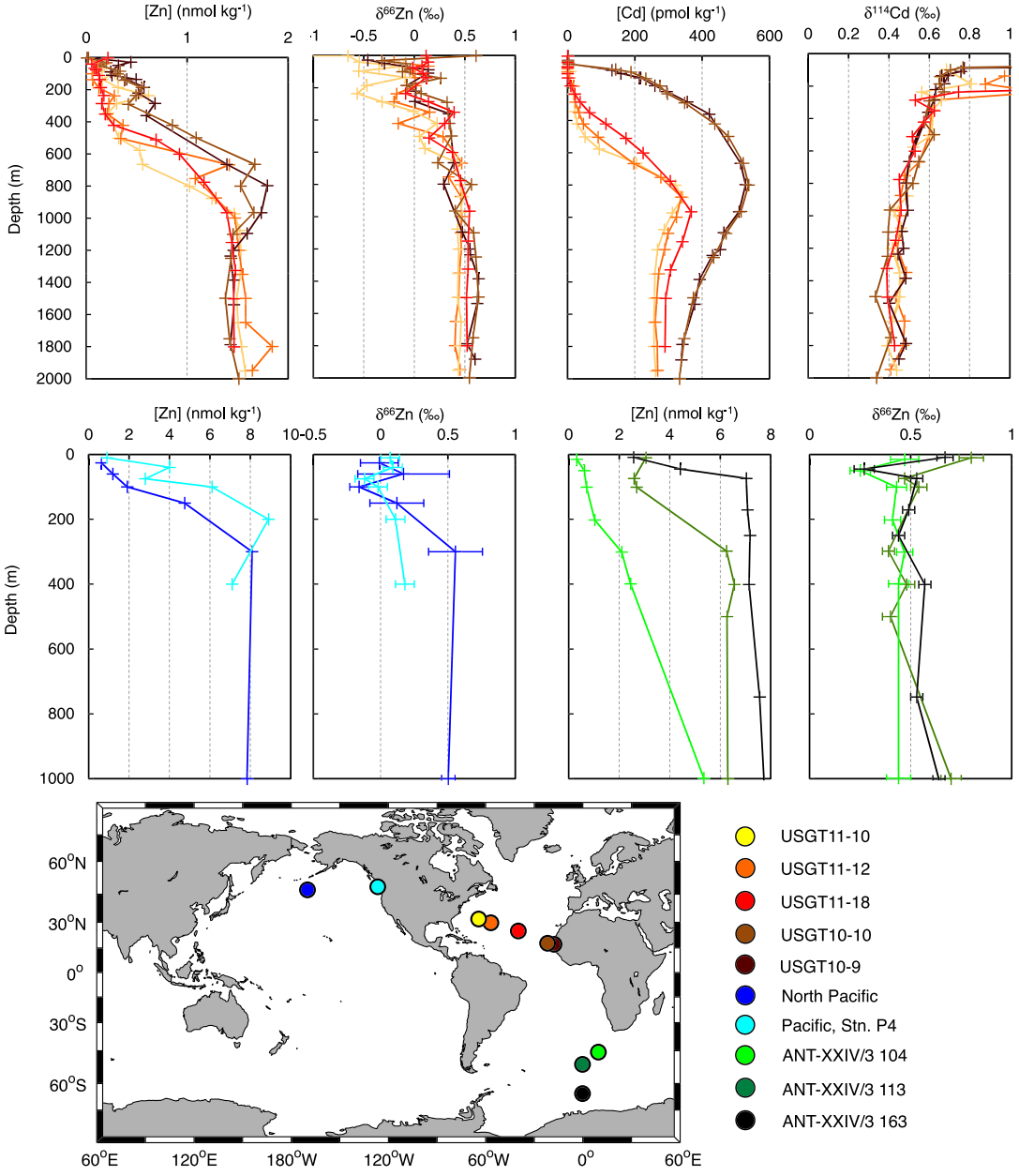

Fig. 1. Zn and Cd concentration and stable isotope profiles from the five locations in the North Atlantic reported here, two previously reported locations in the Pacific including the North Pacific (John, 2007) and station P4 (Bermin et al., 2006) and three locations in Southern Ocean (Zhao et al., 2014). The full North Atlantic data including errors are presented in Table S2.

decrease monotonically towards the surface over the upper 800 m of the water column with a nearly linear relationship to concentrations of N and P. δ^{114}Cd increases monotonically over this same range, consistent with preferential biological assimilation of light Cd isotopes. Zn concentrations also decrease towards the surface, although the decrease is more gradual, similar to Si. δ^{66}Zn has an overall decrease towards the surface. However, in the one case where the surface sample (2 m, station USGT10-10) was of sufficient Zn concentration to allow determination of the stable isotope ratio, δ^{66}Zn increased in the uppermost sample producing a 'negative excursion' in the δ^{66}Zn profile just below the mixed layer. Two published Zn isotope profiles from the North Pacific and two out of three profiles in the Southern Ocean have a similar negative excursion, with lower δ^{66}Zn in the upper thermocline compared to both deeper waters and the surface (Fig. 1; Bermin et al., 2006; John, 2007; Zhao et al., 2014).

Of all the profiles in Fig. 1, North Atlantic waters display the most dramatic sub-surface decreases in δ^{66}Zn and increases in δ^{114}Cd, occurring within North Atlantic Central Water (NACW; above ~600 m) in the western basin (USGT11-10 and -12) and Atlantic Equatorial Water (also above ~600 m) near the African margin. The local nature of these water masses suggests that these features are produced within the North Atlantic, rather than being advected from further away. The extended light δ^{66}Zn signature <600 m close to Bermuda may point to lateral advection of nutrient-depleted Subtropical Mode Waters (STMW; Palter et al., 2005), which form the basis of NACW, which itself may have a light δ^{66}Zn due to scavenging in STMW source regions.

In general, however, simple processes do not easily explain the negative excursions often observed in δ^{66}Zn near the surface. Because the negative excursion is typically observed within the upper 200 m of the water column we conclude that it results

from 1-dimensional vertical processes, rather than being horizontally mixed or advected in from a distant location. The increase in δ^{66}Zn towards the surface can be ascribed to biological uptake of isotopically light Zn. Remineralization of this isotopically light biological material could contribute to the lower δ^{66}Zn below the surface, however our initial expectation is that such remineralization would lead to a monotonic decrease in δ^{66}Zn with depth, as is observed for δ^{114}Cd, rather than the negative excursion which is often observed. Non-steady state processes might also account for the excursion, such as deep mixing which homogenizes δ^{66}Zn over the upper ~200 m, followed by separation of isotopically light and heavy zinc within the upper 200 m due to biological uptake and remineralization. However, if this were the case we would expect δ^{114}Cd to have the same negative excursion in its profile. Finally, it could be that light and heavy Zn isotopes are not released into the dissolved phase at the same rate. This could be due to either the presence of an isotopically-light labile phase within cells and an isotopically heavy refractory phase, or to the scavenging of isotopically heavy Zn onto particles after remineralization.

3.2. Culture data

The concentrations and isotopic compositions of Zn and Cd were monitored within a degrading culture of *Dunalliela tertiolecta* in order to distinguish between the hypothesis that the δ^{66}Zn excursion is caused by sequestration of isotopically heavy Zn within a refractory phase, and the hypothesis that the excursion is caused by scavenging. As much as possible, these experiments were designed to mimic the conditions of the natural ocean. Because our cultures were transferred from non-axenic cultures, we expect that heterotrophic bacterial degradation was the primary pathway for remineralization, as in the real ocean. No synthetic ligand was added to the mixture, but we expect that dissolved organic Zn-binding ligands were be released during bacterial degradation of the cells, as occurs in the natural ocean (Bruland, 1989).

Concentrations of P, Zn, and Cd, and the stable isotope ratios δ^{66}Zn and δ^{114}Cd, were determined in the dissolved, adsorbed and particulate phases over 12 days. P, Zn and Cd concentrations in the particulate phase decreased over the first four days of the experiment, then remained relatively constant until day twelve (Fig. 2), suggesting, that, for each element, there is a labile particulate phase that degrades within the first few days, and a more refractory particulate phase that does not degrade on the timescale of this experiment. The first-order rate constant for release of Zn from the labile organic phase was 1.12 ± 0.12 d^{-1}, which is ~40 times faster than the rate at which Si is released from natural diatoms under similar temperatures and experimental conditions (0.026 d^{-1}) (Lawson et al., 1978). Following dissolution of the labile particulate phase (after day 4), 93% of the released P and 85% of the released Cd remained in the dissolved phase, while only 39% of the released Zn remained in the dissolved phase and 61% was re-adsorbed to particles.

D. tertiolecta preferentially assimilated lighter isotopes of both Cd and Zn from the culture media (Fig. 3). The biological isotope effect for Zn and Cd assimilation were $\Delta\delta^{66}Zn_{\text{plankton-media}} = -0.76 \pm 0.02$‰ and $\Delta\delta^{114}Cd_{\text{plankton-media}} = -0.86 \pm 0.04$‰. Zn isotope fractionation was similar to the −0.8‰ isotope effect observed for the diatom *T. pseudonana* when grown under Zn replete conditions (>1 nmol L^{-1} Zn^{2+}) so that Zn uptake is dominated by a low-affinity transport system (John et al., 2007). Cd isotope fractionation was similar to the -1.36 ± 0.56‰ isotope effect previously measured for the freshwater algae *Chlamydomonas reinhardtii* and *Chlorella* (Lacan et al., 2006). The magnitude of Cd isotope fractionation observed in culture is larger than the −0.2‰ or −0.4‰ fractionations inferred for Southern Ocean phytoplankton in the Weddell Sea and Antarctic Circumpolar Current, respectively

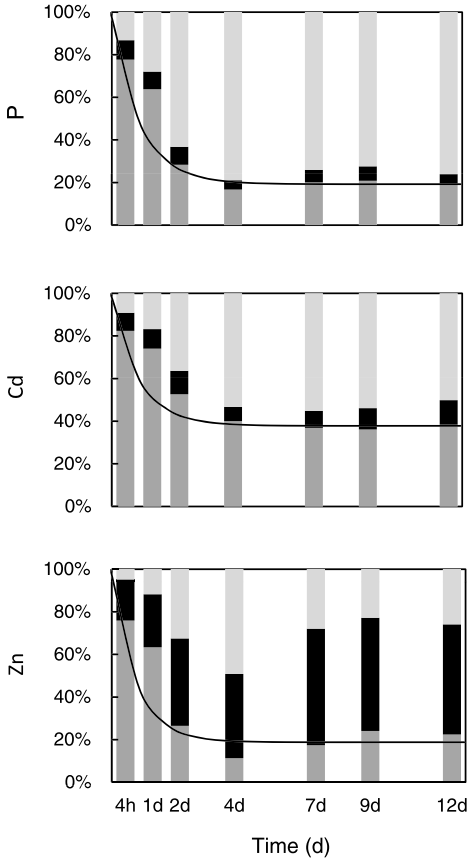

Fig. 2. Relative partitioning of P, Zn, and Cd between the dissolved (light gray), adsorbed (black), and particulate (dark gray) phases in a concentrated suspension of degrading *D. tertiolecta* cells. The rate of particle degradation predicted by assuming that degradation is a first-order process with respect to particle concentration is shown as a black line.

(Abouchami et al., 2011). Differences between Cd isotopic fractionation in nature and in culture could be due either to interspecies variability, or to differences in the uptake pathway employed by phytoplankton at different Cd concentrations, as has been previously observed with Zn (John et al., 2007). We find that Zn and Cd are fractionated by the same relative amount (-24.3 ± 0.6‰ and -23.7 ± 1.1‰ amu amu^{-1}, respectively). This suggests that a similar membrane transporter or physiological mechanism may be involved in isotope fractionation of both Zn and Cd during uptake by phytoplankton. This is consistent with previous observations that Zn and Cd share a transport pathway at high concentrations (Sunda, 2012).

The isotopic composition of both Cd and Zn released from the particulate phase during the degradation experiment was similar to the overall composition of *D. tertiolecta* cells (Fig. 3). Of the Zn released from cells, however, the Zn that remained in the dissolved phase was isotopically lighter than the cells ($\Delta\delta^{66}Zn_{\text{dissolved-plankton}} = -0.27 \pm 0.11$‰), while the Zn that re-adsorbed to organic particles was heavier ($\Delta\delta^{66}Zn_{\text{adsorbed-plankton}} = +0.32 \pm 0.07$‰), throughout the experiment (Fig. 3). The specific mechanisms by which Zn is readsorbed onto particulate material and isotopically fractionated are unknown. However, the extracellular binding of Zn to the diatom *Skeletonema costatum* takes place mostly by coordination to organic carboxylate moieties (Pokrovsky et al., 2005), suggesting that a similar binding may dominate Zn binding to degrading *D. tertiolecta*. Adsorption of inorganic Zn to diatoms has previously been observed to concentrate heavier isotopes on particles with $\Delta\delta^{66}Zn_{\text{adsorbed-dissolved}}$

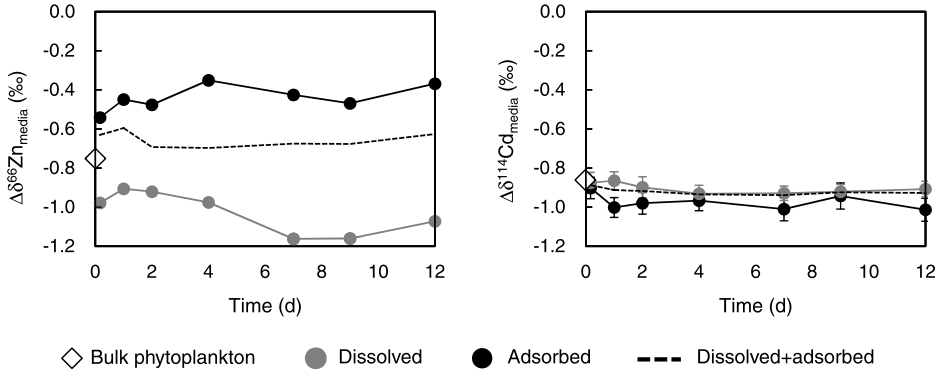

Fig. 3. The isotopic composition of Zn ($\Delta\delta^{66}$Zn) and Cd ($\Delta\delta^{114}$Cd) in a cell suspension of decomposing *D. tertiolecta*, relative to the media in which the phytoplankton were grown (media $\Delta\delta^{66}$Zn and $\Delta\delta^{114}$Cd are defined as 0‰). The isotopic composition of the phytoplankton cells measured in a total digestion of cells at the beginning of the experiment is shown as a white diamond, and the measured isotopic composition of the dissolved and adsorbed phases at each time point are shown as gray and black circles respectively. The isotopic composition of the total metal released from the particles (dissolved + adsorbed), as calculated by mass balance, is shown as a black dashed line. Errors are not shown for the dissolved + adsorbed phase, and are smaller than data points for δ^{66}Zn.

isotope effects of +0.27‰ to +0.43‰ (Gélabert et al., 2006). The slightly larger $\Delta\delta^{66}Zn_{adsorbed\text{-}dissolved}$ of +0.58‰ measured in our experiments is consistent with theoretical predictions for a range of ligands (Black et al., 2011; Fujii and Albarède, 2012; Fujii et al., 2011), perhaps reflecting the organic complexation of dissolved Zn in solution. Adsorbed Zn was released by EDTA-oxalate leaching within 20 min, indicating that Zn exchanges between these phases on a shorter timescale than Zn is released from particles; therefore, we suggest that an equilibrium isotope effect is most likely responsible for the observed fractionation.

These results support the hypothesis that scavenging is responsible for the observed negative excursion in marine δ^{66}Zn profiles. As observed in these experiments, the preferential biological uptake of lighter isotopes in the surface ocean explains the increase in δ^{66}Zn often observed in the surface ocean. The negative excursion in δ^{66}Zn observed below the surface ocean is attributed to preferential loss of isotopically heavy Zn due to scavenging. The alternative hypothesis, that the negative excursions in δ^{66}Zn are due to remineralization of cells containing an isotopically light labile phase and an isotopically heavy refractory phase, are not supported by these experiments. These culture experiments do not provide any evidence of either a refractory soft-tissue biological phase in cultured phytoplankton, or that Zn which remineralizes more slowly has a different isotopic composition than Zn which remineralizes more quickly. Of course, *D. tertiolecta* is not a predominant organism in the natural ocean, and the Zn and Cd concentrations in which the cells were initially grown are much higher than natural concentrations, so the internal cellular storage of Zn and Cd may be different than for open-ocean phytoplankton (Horner et al., 2013). It remains possible that natural phytoplankton do contain an isotopically heavy refractory Zn phase. However, considering that our data are consistent with a hypothesis of Zn scavenging, we are motivated to explore how this process might impact the global biogeochemical cycling of Zn.

3.3. Modeling

Based on the results of degradation experiments and the observed marine profiles of δ^{66}Zn (Figs. 1–3), we hypothesize that scavenging strongly influences the marine distribution of Zn. This hypothesis was tested with a simple 1-dimensional vertical model of Zn and Cd isotope cycling. This model includes the processes of vertical mixing, biological assimilation, regeneration of sinking biological particles and, only for Zn, scavenging. Three parameterizations for Zn scavenging were tested, one in which Zn was adsorbed to biological material and never released ('irreversible scavenging'), one in which Zn was scavenged onto biological par-

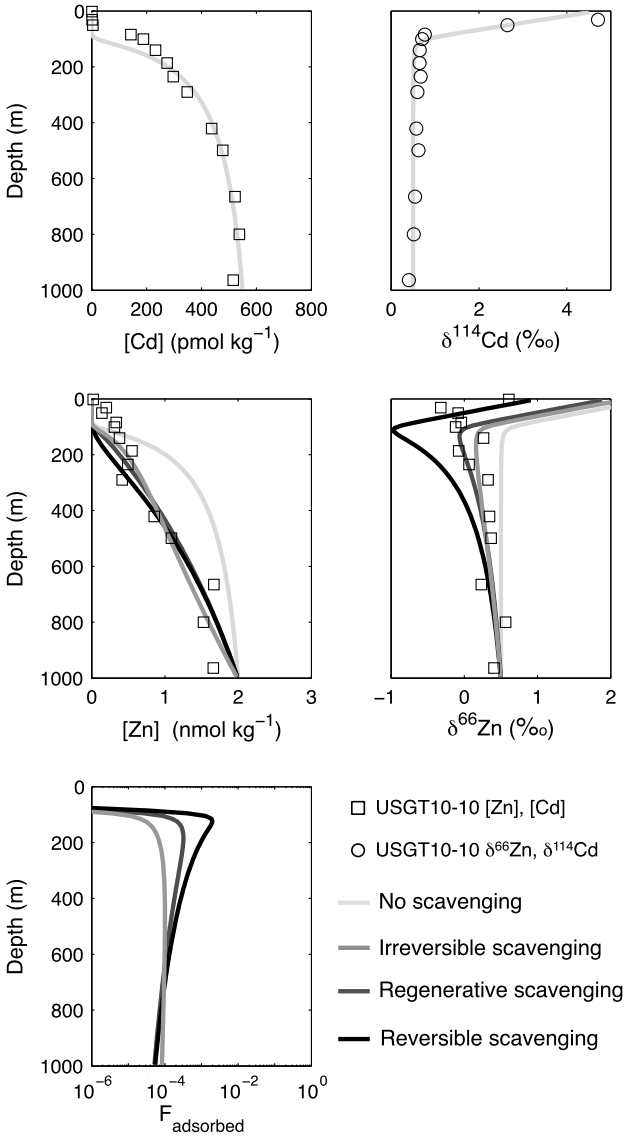

Fig. 4. Modeled Zn and Cd concentrations and stable isotope profiles for runs with no scavenging, irreversible scavenging, regeneration of scavenged Zn from biological particles, and reversible scavenging of Zn onto biological particles, compared to vertical distributions of each from N. Atlantic station USGT10-10, near the African margin. $F_{adsorbed}$ is the fraction of total Zn at each depth found in the adsorbed phase.

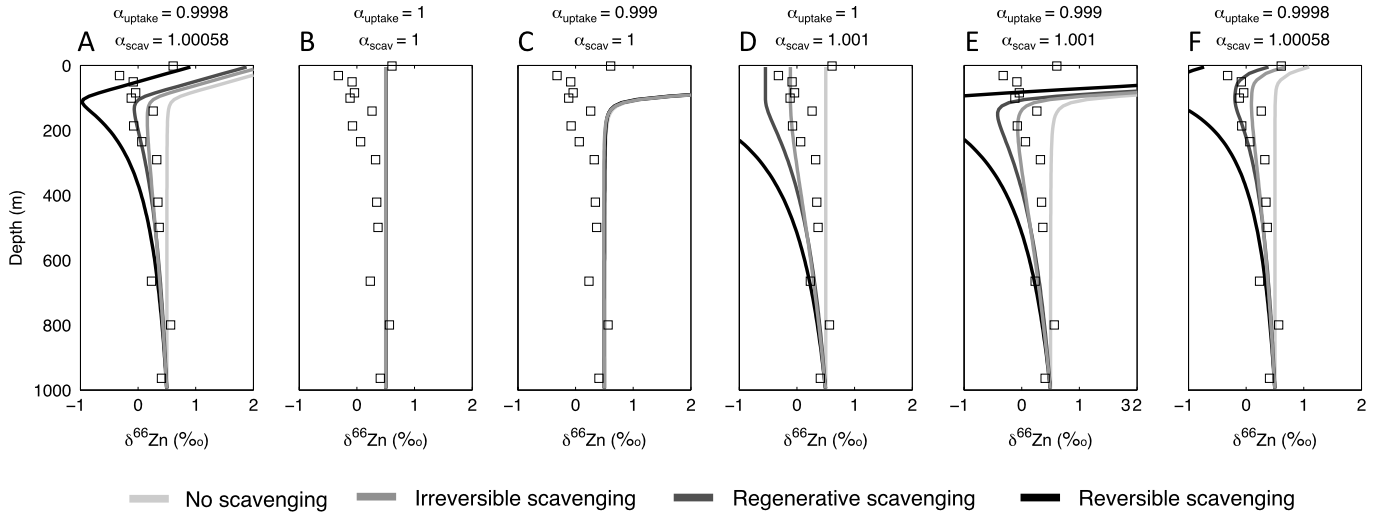

Fig. 5. Model sensitivity analysis for different Zn isotope fractionation factors and Zn uptake rate constants. Model output for estimated natural fractionations of 0.2‰ for Zn uptake and 0.58‰ for Zn scavenging is presented for comparison (A; same as in Fig. 4); with no fractionation during scavenging or uptake, model-predicted δ^{66}Zn does not change (B), with only a 1‰ isotope effect for uptake, δ^{66}Zn increases monotonically towards the surface (C), with only a 1‰ isotope effect for scavenging, δ^{66}Zn decreases monotonically towards the surface (D), with fraction factors of 1‰ for both uptake and scavenging, the magnitude of the δ^{66}Zn excursion increases compared to estimated natural fractionations (E). Applying the estimated natural fractionations, but decreasing the rate constant for Zn uptake by a factor of 1000 decreases the magnitude of the δ^{66}Zn increase above the excursion (F). Besides δ^{66}Zn, all other model output is the same as in Fig. 4.

ticles and released in proportion to the degradation of organic particles ('regenerative scavenging'), and one in which Zn was continually adsorbed and released from sinking particles ('reversible scavenging'). This simple model neglects the effects of horizontal advection. Steady state 1-dimensional models are more appropriate for processes which occur over shorter vertical length scales. Within the upper 1000 m of the North Atlantic, nutrient distributions are greatly influenced by vertical processes, though they also represent the influence of horizontal mixing and advection from the northern North Atlantic and Southern Ocean.

Despite model limitations, it is encouraging that the model reproduces both qualitative and quantitative aspects of the observed δ^{66}Zn profile (Fig. 4). Regardless of the scavenging parameterization used (irreversible, regenerative, or reversible), the model predicts convex upwards-decreasing dissolved δ^{66}Zn towards the top of the thermocline. Close to the surface, within the mixed layer, the model predicts increasing δ^{66}Zn leading to a negative excursion similar to those seen in many natural profiles. The model predicts that less than 1% of the total Zn at any depth (dissolved + particulate) is found in the adsorbed phase for reversible scavenging, less than 0.1% for regenerative scavenging, and less that 0.01% for irreversible scavenging. The fact that Zn scavenging was so much higher (61%) in our culture experiments is most likely a reflection of the much higher particle concentration in culture compared to the open ocean. The model also predicts that throughout the water column the majority of particulate Zn is adsorbed, rather than assimilated, suggesting that the gradual Zn enrichment of deep waters is due to dissolution of adsorbed rather than regenerated assimilated Zn.

Sensitivity analysis of the model shows that only the combined action of scavenging and uptake can produce a negative excursion in δ^{66}Zn (Fig. 5). No change in δ^{66}Zn is observed with α values of 1 (fractionation of 0‰). Isotope fractionation during scavenging alone ($\alpha_{scav} = 1.001$) leads to a monotonic decrease in δ^{66}Zn towards the surface, while fractionation during uptake alone ($\alpha_{scav} = 0.999$) leads to a monotonic increase. Simultaneously increasing amount of isotopic fractionation for both processes to ‰ increases the magnitude of the excursion, but does not change the basic shape of the δ^{66}Zn profile. Finally, we notice that all versions of the model overpredict the increase in δ^{66}Zn at the very surface (above the excursion) compared to the data. A possible explanation for this is that the uptake constant for Zn uptake is set to be equal to the uptake constant for Cd uptake, when in fact it may be that Cd is more readily acquired by phytoplankton in the surface ocean. Indeed, Zn concentrations in the surface ocean are not as depleted as Cd (Fig. 1, Table S2). To account for this we decreased the $k_{assimilation}$ for Zn by a factor of 1000 compared to Cd, thereby decreasing the magnitude of the δ^{66}Zn increase in the uppermost ocean and providing model output more similar to observations.

Based on the sensitivity analysis and the simplicity of our model, and considering that various combinations of parameters reasonably reproduce North Atlantic water-column data, we feel it would be premature to draw conclusions as to which scavenging mechanism is dominant for Zn in the natural ocean (irreversible, regenerative, or reversible). Equally, the magnitude of isotopic fractionation during Zn uptake and scavenging is not yet clear. However the more general conclusions of our modeling, that the combined actions of biological uptake and scavenging can produce δ^{66}Zn profiles similar to those observed in the ocean and that only a small portion of Zn must be in the adsorbed phase at any depth, appear robust.

From the processes observed in a 1-dimensional model of the upper 1000 m at a single station, we can infer the processes that may underlie the global distribution of Zn and δ^{66}Zn. Our model demonstrates that remineralization plus scavenging can cause Zn to be released from sinking particles into the dissolved phase at roughly the same length scale as Si. Even though the processes controlling the dissolution of biogenic Si and Zn are very different, if both elements are nearly completely removed from the dissolved phase in surface waters and both elements are regenerated with the same length scale, their global distribution ought to be similar. Global patterns such as the relative enrichment of both elements in the deep North Pacific compared to the deep North Atlantic and the similar enrichments in specific water masses (e.g. AABW) can therefore be attributed to the similar rates at which Zn and Si are biologically taken up and released from particles, superimposed on the 3-dimensional circulation of the ocean.

4. Conclusions

Scavenging of Zn onto sinking organic matter reconciles previously discordant observations about marine biogeochemical Zn

cycling. The apparent deeper regeneration of Zn in the ocean, compared to Cd and P, is attributable to scavenging of dissolved Zn onto particles, followed by deeper, slower, dissolution of adsorbed Zn, generating depth profiles similar to that of Si. The decrease in dissolved δ^{66}Zn towards the surface, despite uptake of isotopically light Zn into phytoplankton, results from adsorption of isotopically heavy Zn onto particles. δ^{66}Zn profiles in the ocean reflect the varying balance between Zn assimilation and scavenging at different depths in the water column; the negative excursion observed in δ^{66}Zn profiles is explained by the predominance of biological light Zn assimilation in surface waters, and the predominance of scavenging removing heavier isotopes from the thermocline.

Recognizing the importance of Zn scavenging is vital for the development of δ^{66}Zn as a tracer of biogeochemical processes in the ocean. δ^{66}Zn should trace the balance between assimilation and scavenging throughout the oceans, and both processes are strongly influenced by primary productivity. For example, our N. Atlantic data show decreasing δ^{66}Zn towards the surface due to predominant scavenging, while diatom and dissolved δ^{66}Zn in the Southern Ocean have a mixed response to decreasing seawater Zn concentrations, suggesting a more complicated relationship between assimilation and scavenging in this region (Andersen et al., 2011; Zhao et al., 2014). We suggest that δ^{66}Zn, ideally paired with δ^{114}Cd which is not scavenged, may be a useful tracer for constraining changes in the distribution of global phytoplankton productivity for modern climate change, and as a proxy for past global change where shifting productivity influenced glacial–interglacial cycles.

Acknowledgements

This study was funded by NSF grant OCE-1131387. We would like to thank Angela Rosenberg and Beth Bair at the University of South Carolina for technical support with ICPMS analysis, Ed Boyle and Jess Adkins for useful discussions on modeling, and the Captain, Crew and sampling team of the R.V. Knorr on the US GEOTRACES A03 Transect.

Appendix A. Supplementary material

Supplementary material related to this article can be found online at http://dx.doi.org/10.1016/j.epsl.2014.02.053.

References

Abouchami, W., Galer, S.J.G., de Baar, H.J.W., Alderkamp, A.C., Middag, R., Laan, P., Feldmann, H., Andreae, M.O., 2011. Modulation of the Southern Ocean cadmium isotope signature by ocean circulation and primary productivity. Earth Planet. Sci. Lett. 305, 83–91.

Andersen, M.B., Vance, D., Archer, C., Anderson, R.F., Ellwood, M.J., Allen, C.S., 2011. The Zn abundance and isotopic composition of diatom frustules, a proxy for Zn availability in ocean surface seawater. Earth Planet. Sci. Lett. 301, 137–145.

Bacon, M.P., Anderson, R.F., 1982. Distribution of thorium isotopes between dissolved and particulate forms in the deep-sea. J. Geophys. Res., Atmos. 87, 2045–2056.

Bermin, J., Vance, D., Archer, C., Statham, P.J., 2006. The determination of the isotopic composition of Cu and Zn in seawater. Chem. Geol. 226, 280–297.

Black, J.R., Kavner, A., Schauble, E.A., 2011. Calculation of equilibrium stable isotope partition function ratios for aqueous zinc complexes and metallic zinc. Geochim. Cosmochim. Acta 75, 769–783.

Boyle, E.A., 1992. Cadmium and d13C paleochemical ocean distributions during the stage-2 glacial maximum. Annu. Rev. Earth Planet. Sci. 20, 245–287.

Bruland, K.W., 1989. Complexation of zinc by natural organic-ligands in the Central North Pacific. Limnol. Oceanogr. 34, 269–285.

Collier, R., Edmond, J., 1984. The trace-element geochemistry of marine biogenic particulate matter. Prog. Oceanogr. 13, 113–199.

Conway, T.M., Rosenberg, A.D., Adkins, J.F., John, S.G., 2013. A new method for precise determination of iron, zinc and cadmium stable isotope ratios in seawater by double-spike mass spectrometry. Anal. Chim. Acta 793, 44–52.

Cutter, G.A., Bruland, K.W., 2012. Rapid and noncontaminating sampling system for trace elements in global ocean surveys. Limnol. Oceanogr. 10, 425–436.

Ellwood, M.J., Hunter, K.A., 2000. The incorporation of zinc and iron into the frustule of the marine diatom Thalassiosira pseudonana. Limnol. Oceanogr. 45, 1517–1524.

Fujii, T., Albarède, F., 2012. Ab initio calculation of the Zn isotope effect in phosphates, citrates, and malates and applications to plants and soil. PLoS ONE 7, e30726.

Fujii, T., Moynier, F., Pons, M.-L., Albarède, F., 2011. The origin of Zn isotope fractionation in sulfides. Geochim. Cosmochim. Acta 75, 7632–7643.

Gélabert, A., Pokrovsky, O.S., Viers, J., Schott, J., Boudou, A., Feurtet-Mazel, A., 2006. Interaction between zinc and freshwater and marine diatom species: surface complexation and Zn isotope fractionation. Geochim. Cosmochim. Acta 70, 839–857.

Ho, T.-Y., Wen, L.-S., You, C.-F., Lee, D.-C., 2007. The trace metal composition of size-fractionated plankton in the South China Sea: biotic versus abiotic sources. Limnol. Oceanogr. 52, 1776–1788.

Ho, T.-Y., Chou, W.-C., Wei, C.-L., Lin, H.-L., Wong, G.T.F., 2010. Trace metal cycling in the surface water of the South China Sea: vertical fluxes, composition, and sources. Limnol. Oceanogr. 55, 1807–1820.

Horner, T.J., Lee, R.B.Y., Henderson, G.M., Rickaby, R.E.M., 2013. Nonspecific uptake and homeostasis drive the oceanic cadmium cycle. 110, 2500–2505.

John, S.G., 2007. Marine biogeochemistry of zinc isotopes. Jt. Progr. Chem. Oceanogr. Woods Hole Oceanographic Institution/Massachusetts Institute of Technology.

John, S.G., Geis, R.W., Saito, M.A., Boyle, E.A., 2007. Zinc isotope fractionation during high-affinity and low-affinity zinc transport by the marine diatom Thalassiosira oceanica. Limnol. Oceanogr. 52, 2710–2714.

Kunzmann, M., Halverson, G.P., Sossi, P.A., Raub, T.D., Payne, J.L., Kirby, J., 2013. Zn isotope evidence for immediate resumption of primary productivity after snowball Earth. Geology 41, 27–30.

Lacan, F., Francois, R., Ji, Y.C., Sherrell, R.M., 2006. Cadmium isotopic composition in the ocean. Geochim. Cosmochim. Acta 70, 5104–5118.

Lawson, D.S., Hurd, D.C., Pankratz, H.S., 1978. Silica dissolution rates of decomposing phytoplankton assemblages at various temperatures. Am. J. Sci. 278, 1373–1393.

Lee, B.G., Fisher, N.S., 1992. Degradation and elemental release rates from phytoplankton debris and their geochemical implications. Limnol. Oceanogr. 37, 1345–1360.

Little, S.H., Vance, D., Siddall, M., Gasson, E., 2013. A modeling assessment of the role of reversible scavenging in controlling oceanic dissolved Cu and Zn distributions. Glob. Biogeochem. Cycles 27, 1–12.

Lohan, M.C., Statham, P.J., Crawford, D.W., 2002. Total dissolved zinc in the upper water column of the subarctic North East Pacific. Deep-Sea Res., Part 2, Top. Stud. Oceanogr. 49, 5793–5808.

Marchitto, T.M., Lynch-Stieglitz, J., Hemming, S.R., 2005. Deep pacific $CaCO_3$ compensation and glacial–interglacial atmospheric CO_2. Earth Planet. Sci. Lett. 231, 317–336.

Marchitto, T.M., Oppo, D.W., Curry, W.B., 2002. Paired benthic foraminiferal Cd/Ca and Zn/Ca evidence for a greatly increased presence of Southern Ocean Water in the glacial North Atlantic. Paleoceanography 17.

Maréchal, C.N., Nicolas, E., Douchet, C., Albarède, F., 2000. Abundance of zinc isotopes as a marine biogeochemical tracer. Geochem. Geophys. Geosyst. 1. 1999GC000029.

Martin, J.H., Knauer, G.A., Karl, D.M., Broenkow, W.W., 1987. VERTEX – carbon cycling in the Northeast Pacific. Deep-Sea Res., A, Oceanogr. Res. Pap. 34, 267–285.

Morel, F.M.M., Reinfelder, J.R., Roberts, S.B., Chamberlain, C.P., Lee, J.G., Yee, D., 1994. Zinc and carbon co-limitation of marine phytoplankton. Nature 369, 740–742.

Morel, F.M.M., Rueter, J.G., Anderson, D.M., Guillard, R.R.L., 1979. AQUIL: a chemically defined phytoplankton medium for trace metal studies. J. Phycol. 15, 135–141.

Palter, J.B., Lozier, M.S., Barber, R.T., 2005. The effect of advection on the nutrient reservoir in the North Atlantic subtropical gyre. Nature 437, 687–692.

Pichat, S., Douchet, C., Albarède, F., 2003. Zinc isotope variations in deep-sea carbonates from the eastern equatorial Pacific over the last 175 ka. Earth Planet. Sci. Lett. 210, 167–178.

Pokrovsky, O.S., Pokrovski, G.S., Gelabert, A., Schott, J., Boudou, A., 2005. Speciation of Zn associated with diatoms using X-ray absorption spectroscopy. Environ. Sci. Technol. 39, 4490–4498.

Ripperger, S., Rehamper, M., Porcelli, D., Halliday, A.N., 2007. Cadmium isotope fractionation in seawater – a signature of biological activity. Earth Planet. Sci. Lett. 261, 670–684.

Sarmiento, J.L., Gruber, N., Brzezinski, M.A., Dunne, J.P., 2004. High-latitude controls of thermocline nutrients and low latitude biological productivity. Nature 427, 56–60.

Sarmiento, J.L., Simeon, J., Gnanadesikan, A., Gruber, N., Key, R.M., Schlitzer, R., 2007. Deep ocean biogeochemistry of silicic acid and nitrate. Glob. Biogeochem. Cycles 21, GB1S90.

Shaked, Y., Xu, Y., Leblanc, K., Morel, F.M.M., 2006. Zinc availability and alkaline phosphatase activity in Emiliania huxleyi: implications for Zn–P co-limitation in the ocean. Limnol. Oceanogr. 51, 299–309.

Shiller, A.M., Boyle, E., 1985. Dissolved zinc in rivers. Nature 317, 49–52.

Sunda, W.G., 2012. Feedback interactions between trace metal nutrients and phytoplankton in the ocean. Front. Microbiol. 3. Article 204.

Sunda, W.G., Huntsman, S.A., 1992. Feedback interactions between zinc and phytoplankton in seawater. Limnol. Oceanogr. 37, 25–40.
Sunda, W.G., Price, N.M., Morel, F.M.M., 2005. Trace metal ion buffers and their use in culture studies. In: Algal Culturing Techniques, pp. 35–64.
Twining, B.S., Baines, S.B., Fisher, N.S., 2004. Element stoichiometries of individual plankton cells collected during the Southern Ocean Iron Experiment (SOFeX). Limnol. Oceanogr. 49, 2115–2128.
Twining, B.S., Baines, S.B., Fisher, N.S., Maser, J., Vogt, S., Jacobsen, C., Tovar-Sanchez, A., Sanudo-Wilhelmy, S.A., 2003. Quantifying trace elements in individual aquatic protist cells with a synchrotron X-ray fluorescence microprobe. Anal. Chem. 75, 3806–3816.
Zhao, Y., Vance, D., Abouchami, W., de Baar, H.J.W., 2014. Biogeochemical cycling of zinc and its isotopes in the Southern Ocean. Geochim. Cosmochim. Acta 125, 653–672.